

A Meshless Method for Retrieving Nonlinear Large External Forces on Euler-Bernoulli Beams

Chih-Wen Chang*

Department of Mechanical Engineering, National United University, Miaoli, 360302, Taiwan

*Corresponding Author: Chih-Wen Chang. Email: cwchang@nuu.edu.tw

Received: 08 January 2022; Accepted: 11 March 2022

Abstract: We retrieve unknown nonlinear large space-time dependent forces burdened with the vibrating nonlinear Euler-Bernoulli beams under varied boundary data, comprising two-end fixed, cantilevered, clamped-hinged, and simply supported conditions in this study. Even though some researchers used several schemes to overcome these forward problems of Euler-Bernoulli beams; however, an effective numerical algorithm to solve these inverse problems is still not available. We cope with the homogeneous boundary conditions, initial data, and final time datum for each type of nonlinear beam by employing a variety of boundary shape functions. The unknown nonlinear large external force can be recuperated via back-substitution of the solution into the nonlinear Euler-Bernoulli beam equation when we acquire the solution by utilizing the boundary shape function scheme and deal with a small-scale linear system to gratify an additional right-side boundary data. For the robustness and accuracy, we reveal that the current schemes are substantiated by comparing the recuperated numerical results of four instances to the exact forces, even though a large level of noise up to 50% is burdened with the overspecified conditions. The current method can be employed in the online real-time computation of unknown force functions in space-time for varied boundary supports of the vibrating nonlinear beam.

Keywords: Inverse problems; nonlinear Euler-Bernoulli beams; ill-posed problems; nonlinear space-time dependent force; boundary shape functions

1 Introduction

As we all know, retrieving external forces of Euler-Bernoulli beams plays very important roles in many engineering and scientific areas. These equations occur in the vibration of a structure, the cutting process in engineering, the sandwiches beams, the cable-stayed beams, the rotating beams, the aircraft engineering, the design of mechanical cutting tools, the nondestructive testing and so forth.

For linear external forces of linear Euler-Bernoulli equations, Han et al. [1] tested four approximate models for a transversely vibrating beam: the Euler-Bernoulli, Rayleigh, shear, and Timoshenko



This work is licensed under a Creative Commons Attribution 4.0 International License, which permits unrestricted use, distribution, and reproduction in any medium, provided the original work is properly cited.

models. For each model, the orthogonality data were identified, and the forced response was acquired employing the approach of eigenfunction expansion. Nevertheless, they only displayed one example to discuss the second frequency spectrum. Later, expressions for the maximum cutting force, variation of the cutting force in one complete rotation, surface quality and many other characteristics of the cutting force components can be derived from the proposed cutting force model [2]. The results can be shown in charts to permit machining operators to easily choose the cutting data. Abu-Hilal [3] employed Green functions to decide the dynamic response of damped Euler–Bernoulli beams and demonstrate the dynamic behavior of single and multi-span beams, single and multi-loaded beams; however, he did not show the robustness of the proposed method. Then, Andr n et al. [4] demonstrated that the clamped boring bar has non-linear dynamic properties. They also showed that non-linearities can be reduced by modifying the clamping of the boring bar. Nevertheless, they did not display the comparisons with the other literature. After that, Yoon et al. [5] used a mechanistic cutting force model to prophesy the cutting process. The experimental coefficient modelling scheme was developed for the formulation of theoretical cutting force by pondering the specific cutting force coefficient. Later, Gradi sek et al. [6] presented expressions for semi-empirical mechanistic identification of specific cutting and edge force coefficients for a general helical end mill from milling tests at an arbitrary radial immersion. Apart from that, Nicaise et al. [7] pondered two inverse issues of deciding point sources in vibrating beams by boundary measurements. They displayed that the boundary observation at one extremity of the area decides uniquely the sources for an arbitrarily small time of observation. The output-feedback controller for an undamped shear beam was proposed by Krstic et al. [8,9]. Then, Hasanov [10] formulated new classes of inverse source problems for vibrating cantilevered elastic beams, within the range of Euler–Bernoulli beam theory. This result showed the iteration parameter via the Lipschitz constant in gradient-type methods, which were mostly employed in the numerical implementation of inverse issues. Later, Huang et al. [11] dealt with an inverse forced vibration issue, based on the conjugate gradient method (CGM), which was tested in this study to evaluate the unknown spatial and temporal-dependent external forces for the cutting tools by using the simulated beam displacement measurements. The numerical experiments were performed to test the validity of the CGM by utilizing varied types of external forces and measurement errors. After that, Liu [12] recovered an unknown space–time-dependent force in an Euler–Bernoulli beam vibration equation by an effective combination of the Lie-group adaptive approach and the differential quadrature scheme through a few iterations. Then, Kawano [13] analyzed the issue of the identification of the distribution of asynchronous vibration sources and rigidity perturbations in Euler–Bernoulli beams. Hasanov et al. [14] presented that the collocation method combined with the truncated singular value decomposition was used to estimate the degree of ill-posedness of the pondered inverse source issue. The numerical results illustrated bounds of applicability of the proposed algorithm, also its efficiency and accuracy. Later, Hasanov et al. [15] solved these two inverse issues related to asynchronous load identification that have significant engineering applications. Note that when in some inverse issues the use of boundary data was desirable or a necessity, as in the chief example of electric impedance tomography. After that, an adjoint problem approach was used for a class of inverse issues related to the identification of temporal and spatial load distributions in the Euler–Bernoulli beam equation [16]; furthermore, they claimed that the constructed iterative algorithm was robust, which allowed the use of random noisy data up to 10% noise level. However, the numerical results with noisy data are not good. Maciag et al. [17] addressed an approximate scheme of solving direct and inverse problems described by Bernoulli–Euler inhomogeneous equation of vibrations of a beam; nevertheless, they did not show the robustness of their algorithm.

For the free vibration of composite beams and non-uniform beams, Liu et al. [18] proposed a new upper bound theory to estimate the first few natural frequencies. They addressed the inverse problems of composite beam equations, where they used the orthogonal system of boundary functions as bases to expand the unknown functions and derived linear algebraic equations to decide the expansion coefficients. The robustness of the current inversion approaches was shown by numerical instances. Then, when adjoint eigenfunctions were adopted as the test functions in Green's second identity for the Euler-Bernoulli beam equation, they can develop a simple noniterative numerical method to retrieve an unknown space-dependent external force exerted on the beam [19]. Therefore, they had a noniterative algorithm to retrieve the unknown force supplemented by the noisy final time displacement data. Later, Liu et al. [20] resolved the inverse source issue of a nonlinear wave equation, developing a family of m -order homogenization functions. This method did not require the iteration to resolve nonlinear equations, which was accurate for simultaneously solving the solution. Then, Liu et al. [21] addressed the higher-dimensional inverse heat source issues of nonlinear convection-diffusion reaction equations in 2-D rectangles and 3-D cuboids, of which the final time data and the Neumann boundary conditions on one-side were over-specified. Numerical exams found that the new approach was very accurate to reveal the solution. After that, Bajkowski et al. [22] contemplated a theoretical analysis and experimental examination of a sandwich beam, with a core layer made of controllable material that can change its properties over time. Numerical simulations were performed to study the possibility of shifting beam vibration frequency towards ranges distant from resonance; however, they did not display the robustness of their scheme. Apart from that, Liu et al. [23] developed a simple and effective numerical skill, which aimed to accurately and quickly deal with thin plate bending issues. Note that the proposed algorithm is quite accurate for the thin plate, the clamped plate, and the simply supported plate problems. The nonlinear primary resonance in the vibration control of cable-stayed beam with time delay feedback was studied by [24]. The numerical simulation was also given to determine the optimal value for control gain and time delays that can improve the vibrations suppression efficiency; nevertheless, this approach is complex and does not discuss the noisy effect. Later, Li et al. [25] mentioned that very few results were reported on the vibration issues of some novel multilayer sandwich structures with lattice truss cores in the literature. Contributions of this literature lie in the development of the new deformation relations of multilayer sandwich beams, the construction of the dynamic models, and the systematic analysis of vibration characteristics with both the numerical and experimental schemes. Apart from that, the nonlinear free vibration and principal parametric resonance of rotating beams were investigated taking into account the lagging-axial coupling motion because of Coriolis force [26]. The nonlinear equations of motion were obtained through a direct Lagrangian formulation. Later, Liu et al. [27] recovered unknown space-time-dependent forces imposed on the vibrating Euler-Bernoulli beams under varied boundary conditions. The accuracy and robustness of the present schemes were confirmed by comparing the retrieved results of several instances to the exact forces, even though considerable noise was shown in the overspecified data.

For the difficult nonlinear Euler-Bernoulli beams, Barari et al. [28] proposed the variational iteration method and parametrized perturbation method to study the non-linear vibration of beams and nonlinear responses of a clamped-clamped buckled beam. However, they did not show the robustness of their approaches and mechanical affairs. Then, Weeger et al. [29] analyzed the vibrations of nonlinear structures by means of the new method of isogeometric finite elements. Nevertheless, they did not demonstrate real applications and the noisy effect of their schemes. Kitarovic [30] resolved a nonlinear kinematics of the 2-D, non-shear-deformable and extensible Euler-Bernoulli beam imposed with the planar flexure and/or lengthening/shortening. He discussed implications of the derived

formulations pertinent to the progressive collapse analysis methods based on the Smith's approach; however, the 2-D issue was merely considered. After that, Bagheri et al. [31] coped with nonlinear responses of a clamped-clamped buckled beam to certify the vibrational behaviors of beam. They claimed that comparing with numerical results, note that the approximate solutions were in good agreement with the analytical solutions. On the other hand, about the recent nonlinear dynamical mathematical modeling and its applications, Raza and his coworkers have proposed many schemes to tackle those issues, such as the nonlinear stochastic leprosy epidemic model [32], the cervical cancer epidemic model [33], the dynamics of the pneumonia-like infections of epidemic models [34], the cancer virotherapy model [35], the pine wilt epidemic model [36], and dynamical analysis of coronavirus disease with crowding effect, and vaccination [37].

This article is arranged as follows. Section 2 displays the nonlinear problem statement and constructs the new boundary shape function, and homogeneous boundary data of the beam. In Section 3, we acquire shape functions and introduce a free parameter into the boundary shape function, which leads to a variety of boundary shape functions. Four numerical examples of the nonlinear large external forces on vibrating nonlinear Euler-Bernoulli beams are shown in Section 4. At last, we display the conclusions in Section 5.

2 Problem Statement and Establishment of Boundary Shape Function

We deliberate an inverse source issue to reveal an unknown nonlinear force function $H(x, t)$ being burdened with a vibrating nonlinear Euler-Bernoulli beam with varied boundary supports. It is a severely ill-posed problem in the engineering field. The nonlinear beam with simply supported boundary data is utilized as the first significant instance, for which the pair of unknown functions $\langle v(x, t), H(x, t) \rangle$ concurrently gratifies

$$v_{tt}(x, t) + \beta v_{xxxx}(x, t) + v^2(x, t) = H(x, t), (x, t) \in \Gamma, \quad (1)$$

$$v(x, 0) = d(x), v_t(x, 0) = g(x), 0 < x < \ell, \quad (2)$$

$$v(0, t) = 0, v_{xx}(0, t) = 0, v(\ell, t) = 0, v_{xx}(\ell, t) = 0, t \in [0, t_f], \quad (3)$$

where $\Gamma := \{(x, t) | 0 < x < \ell, 0 < t \leq t_f\}$, $\beta := EI/(\kappa A)$ is a constant with Young's modulus E , I the moment of inertia, κ is the material density, and A is the cross-sectional area.

It cannot be resolved forthrightly to reveal $v(x, t)$ since the problem (1)–(3) has an unknown nonlinear force function $H(x, t)$. To retrieve $H(x, t)$ and deal with $v(x, t)$ in the entire area, we clarify the additional conditions of

$$v(x, t_f) = h(x), \quad (4)$$

$$v_x(\ell, t) = \tau(t), \quad (5)$$

First of all, we deliberate a partial boundary shape function in the time orientation:

$$D^0(x, t) = \left(1 - \frac{t^2}{t_f^2}\right) d(x) + \frac{t^2}{t_f^2} h(x) + \left(t - \frac{t^2}{t_f}\right) g(x), \quad (6)$$

which gratifies the conditions (2) and (4):

$$D^0(x, 0) = d(x), D_t^0(x, 0) = g(x), D^0(x, t_f) = h(x). \quad (7)$$

Assuming

$$D^0(x, t) \neq 0, \tag{8}$$

which denotes that the functions $d(x)$, $g(x)$, and $h(x)$ cannot be zeros concurrently.

Next, we search four polynomial-type shape functions $c_p(x), p = 1, \dots, 4$, gratifying

$$c_1(0) = 1, c_1'(0) = 0, c_1(l) = 0, c_1'(l) = 0, \tag{9}$$

$$c_2(0) = 0, c_2''(0) = 1, c_2(l) = 0, c_2''(l) = 0, \tag{10}$$

$$c_3(0) = 0, c_3''(0) = 0, c_3(l) = 1, c_3'(l) = 0, \tag{11}$$

$$c_4(0) = 0, c_4''(0) = 0, c_4(l) = 0, c_4'(l) = 1. \tag{12}$$

We find that those four boundary data in Eq. (3) of the simply supported beam can be gratified by a nonzero boundary shape function:

$$D(x, t) = D^0(x, t) - c_1(x)D^0(0, t) - c_2(x)D_{xx}^0(0, t) - c_3(x)D^0(l, t) - c_4(x)D_{xx}^0(l, t). \tag{13}$$

We can acquire through some calculations

$$c_1(x) = 1 + \left(\frac{x}{l}\right)^4 - 2\left(\frac{x}{l}\right)^3, \tag{14}$$

$$c_2(x) = \frac{x^2}{2} + \frac{l^2}{3}\left(\frac{x}{l}\right)^4 - \frac{5l^2}{6}\left(\frac{x}{l}\right)^3, \tag{15}$$

$$c_3(x) = -\left(\frac{x}{l}\right)^4 + 2\left(\frac{x}{l}\right)^3, \tag{16}$$

$$c_4(x) = -\frac{l^2}{6}\left(\frac{x}{l}\right)^3 + \frac{l^2}{6}\left(\frac{x}{l}\right)^4. \tag{17}$$

We can verify that the boundary shape function $D(x, t)$ gratifies by employing the compatibility data,

$$D(x, 0) = d(x), D_t(x, 0) = g(x), D(x, t_f) = h(x), \tag{18}$$

$$D(0, t) = 0, D_{xx}(0, t) = 0, D(l, t) = 0, D_{xx}(l, t) = 0. \tag{19}$$

3 Combination of Boundary Shape Functions

The boundary shape function $D(x, t)$ is completely decided by the shape functions $c_p(x), p = 1, \dots, 4$, initial data, and the terminal time condition of $v(x, t)$ in the area Ψ . We can generalize $D(x, t)$ and use it to the beam Eq. (1) by bringing in a new scheme. For the inverse source issue of the beam equation, we utilize the superposition of the varied order boundary shape functions to deal with it.

Note that we do not utilize the basis of the solution since there subsists no free parameter in $D(x, t)$ although $D(x, t)$ is well constructed. We employ the q th-order shape functions $c_p(q, x), p = 1, \dots, 4$ to generalize Eqs. (9)–(17), which are decided by

$$c_1(q, 0) = 1, c_1''(q, 0) = 0, c_1(q, l) = 0, c_1'(q, l) = 0, \tag{20}$$

$$c_2(q, 0) = 0, c_2''(q, 0) = 1, c_2(q, l) = 0, c_2''(q, l) = 0, \tag{21}$$

$$c_3(q, 0) = 0, c_3''(q, 0) = 0, c_3(q, \ell) = 1, c_3''(q, \ell) = 0, \quad (22)$$

$$c_4(q, 0) = 0, c_4''(q, 0) = 0, c_4(q, \ell) = 0, c_4''(q, \ell) = 1. \quad (23)$$

We can acquire through some calculations

$$c_1(q, x) = 1 + \frac{q+1}{2} \hat{u}^{q+3} - \frac{q+3}{2} \hat{u}^{q+2}, \quad (24)$$

$$c_2(q, x) = \frac{x^2}{2} + \frac{\ell^2 q(q+3)}{4(q+2)} \hat{u}^{q+3} - \frac{\ell^2 (q+1)(q+4)}{4(q+2)} \hat{u}^{q+2}, \quad (25)$$

$$c_3(q, x) = -\frac{q+1}{2} \hat{u}^{q+3} + \frac{q+3}{2} \hat{u}^{q+2}, \quad (26)$$

$$c_4(q, x) = -\frac{\ell^2}{2(q+2)} \hat{u}^{q+2} + \frac{\ell^2}{2(q+2)} \hat{u}^{q+3}, \quad (27)$$

where the normalized coordinate \hat{u} is clarified on

$$\hat{u} = \frac{x}{\ell}. \quad (28)$$

We can induce $D(x, t)$ in Eq. (13) to boundary shape functions as follows:

$$D(q, x, t) = D^0(q, x, t) - c_1(q, x) D^0(q, 0, t) - c_2(q, x) D_{xx}^0(q, 0, t) \\ - c_3(q, x) D^0(q, \ell, t) - c_4(q, x) D_{xx}^0(q, \ell, t), \quad (29)$$

in which

$$D^0(q, x, t) = (1 - \tilde{\delta}^{q+1})d(x) + \tilde{\delta}^{q+1}h(x) + t_f(\tilde{\delta} - \tilde{\delta}^{q+1})g(x), \quad (30)$$

$$\tilde{\delta} = \frac{t}{t_f}. \quad (31)$$

These conditions are gratified can be confirmed easily as follows:

$$D(q, x, 0) = d(x), D_t(q, x, 0) = g(x), D(q, x, t_f) = h(x), \quad (32)$$

$$D(q, 0, t) = 0, D_{xx}(q, 0, t) = 0, D(q, \ell, t) = 0, D_{xx}(q, \ell, t) = 0. \quad (33)$$

4 Numerical Scheme and Experiments

Assuming

$$v(x, t) = \sum_{q=1}^s a_q D(q, x, t), \quad (34)$$

where a_q are unknown coefficients to be chosen, and $D(q, x, t)$, $q = 1, \dots, s$ are nonzero bases described by Eq. (31).

The strain data $\tau(t) = v_x(\ell, t)$ are demonstrated in Eq. (5). Therefore, we obtain the following equation by using the differential of Eq. (36) with respect to x and introducing $x = \ell$

$$\sum_{q=1}^s a_q D_x(q, \ell, t) = \tau(t). \quad (35)$$

The linear equations can be acquired by collocating points $t_p = pt_f/w, p = 1, \dots, w$ to gratify Eq. (37):

$$\sum_{q=1}^s a_q D_x(q, l, t_p) = \tau(t_p), p = 1, \dots, w, \tag{36}$$

$$\sum_{q=1}^s a_q = 1, \tag{37}$$

in which the last equation is accustomed to promise that $v(x, t)$ in Eq. (34) can gratify the conditions in Eqs. (2)–(4).

We can decide the s weight coefficients $a_q, q = 1, \dots, s$ by resolving the $w_s = w + 1$ linear Eqs. (36) and (37). Eq. (34) can be used to cope with $v(x, t)$ in the entire area. By back substituting $v(x, t)$ into Eq. (1), we can retrieve $H(x, t)$ by

$$H(x, t) = \sum_{q=1}^s a_q D_{ii}(q, x, t) + \beta \sum_{q=1}^s a_j D_{xxxx}(q, x, t). \tag{38}$$

By utilizing the boundary shape functions method (BSFM), we can reveal that this present scheme is suitable to solve the inverse source issue of the beam equation. In fact, s is a small number, as shown then, such that we merely require to address a s -dimensional small-scale normal linear system to retrieve $H(x, t)$.

Eqs. (4) and (5) are often contaminated by random noise:

$$\hat{h}(x) = h(x) + rK(x), \hat{\tau}(t) = \tau(t) + rK(t), \tag{39}$$

where $K(x), K(t) \in [-1, 1]$ are random functions and r is the intensity of noise effective.

While the maximum values of $|h(x)|$ and $|\tau(t)|$ are large, adding noise with a small value r might be nonsensical. Therefore, in place of Eq. (39), in some situations, noise disturbance with a relative intensity ξ can be pondered:

$$\hat{h}(x) = h(x) + \xi|h(x)|K(x), \hat{\tau}(t) = \tau(t) + \xi|\tau(t)|K(t). \tag{40}$$

Employing Eqs. (1)–(5) to retrieve the unknown space-time dependent force $H(x, t)$ is a complicated work since the system (1)–(5) is severely underdetermined and the resulting inverse source issue is very ill-posed.

All the computational schemes were implemented to the Fortran code on the Microsoft Developer Studio platform in OS Windows 10 (64 bit) with i3-4160 3.60 GHz CPU and 16 GB memory.

4.1 Example 1 of A Simply Supported Beam

In the following four numerical examples, we usually choose the absolute error

$$|H_w(x_q, t_q) - H(x_q, t_q)|$$

to evaluate the accuracy of a numerical solution, where $H_w(x_q, t_q)$ and $H(x_q, t_q)$ are the numerically retrieved force and the exact force at M points $(x_q, t_q), q = 1, \dots, M$, respectively. To ponder a relative root-mean-square error defined by

$$e(H) = \sqrt{\frac{\sum_{q=1}^M [H_w(x_q, t_q) - H(x_q, t_q)]^2}{\sum_{q=1}^M H^2(x_q, t_q)}}$$

to evaluate the accuracy of numerically retrieved force.

We deliberate a complicated space-time-dependent force generated from

$$v(x, t) = e^{2t} [1000 (3x^5 - 5x^4 + 2x) + \sin(2\pi x)] + \pi t(x^4 - 2x^3 + x), \quad (41)$$

from which we find that the force to be retrieved is nonseparable and complicated.

The noise is $r = 0.9$, and we take $\beta = 0.5$. We utilize the BSFM with $s = 5$ and $w = 500$. Comparing the numerically retrieved solution of $H(x, t)$ with the exact force $H(x, t)$, as displayed in Figs. 1a and 1c. We also demonstrate the maximum errors (MEs) of $v(x, t)$ and the recovery of $H(x, t)$ under the noisy effect in Fig. 2. Great results are acquired with the MEs over the plane $[0, 1] \times (0, 1]$ being 2.89×10^{-2} for $v(x, t)$ and 284.5 for $H(x, t)$. We also obtain the maximum absolute value of $H(x, t)$ over the plane $[0, 1] \times (0, 1]$ is 3.47×10^7 , and $e(H) = 7.44 \times 10^{-6}$ is very small.

Considering a large relative noise of $\xi = 0.01$ in Eq. (40), we employ the BSFM with $s = 2$ and $w = 500$ to retrieve $H(x, t)$, as shown in Fig. 1b. The accuracy lost three orders compared with the aforementioned results, where the ME for $v(x, t)$ is 43.67, the ME for $H(x, t)$ is 519282.27, and $e(H) = 9.87 \times 10^{-3}$. For this example, the CPU time is less than 1.0 s.

4.2 Example 2 of A Clamped-hinged Beam

We show that the clamped-hinged beam owns the boundary data, shape functions, and boundary shape functions as follows:

$$v(0, t) = 0, v_x(0, t) = 0, v(l, t) = 0, v_{xx}(l, t) = 0, \quad (42)$$

$$\begin{aligned} c_1(q, x) &= 1 + \frac{q}{2} \bar{x}^{q+2} - \frac{q+2}{2} \bar{x}^{q+1}, \\ c_2(q, x) &= x + \frac{q}{2l} \bar{x}^{q+2} - \frac{q+2}{2l} \bar{x}^{q+1}, \\ c_3(q, x) &= -\frac{q}{2} \bar{x}^{q+2} + \frac{q+2}{2} \bar{x}^{q+1}, \\ c_4(q, x) &= -\frac{l^2}{2(q+1)} \bar{x}^{q+1} + \frac{l^2}{2(q+1)} \bar{x}^{q+2}, \end{aligned} \quad (43)$$

$$\begin{aligned} D(q, x, t) &= D^0(q, x, t) - c_1(q, x)D^0(q, 0, t) - c_2(q, x)D^0_x(q, 0, t) \\ &\quad - c_3(q, x)D^0(q, l, t) - c_4(q, x)D^0_{xx}(q, l, t), \end{aligned} \quad (44)$$

where $D^0(q, x, t)$ is described utilizing Eq. (30).

We ponder a complicated space-time-dependent force of the clamped-hinged beam produced from

$$\begin{aligned} v(x, t) &= 2000e^t (3x^5 - 7x^4 + 4x^3) + 2 \cos(\pi t) [4\pi (x^2 - x) \\ &\quad - (\pi^2 + 2\pi) (x^3 - x^2) + 4 \exp[\sin(\pi x)] - 4]. \end{aligned} \quad (45)$$

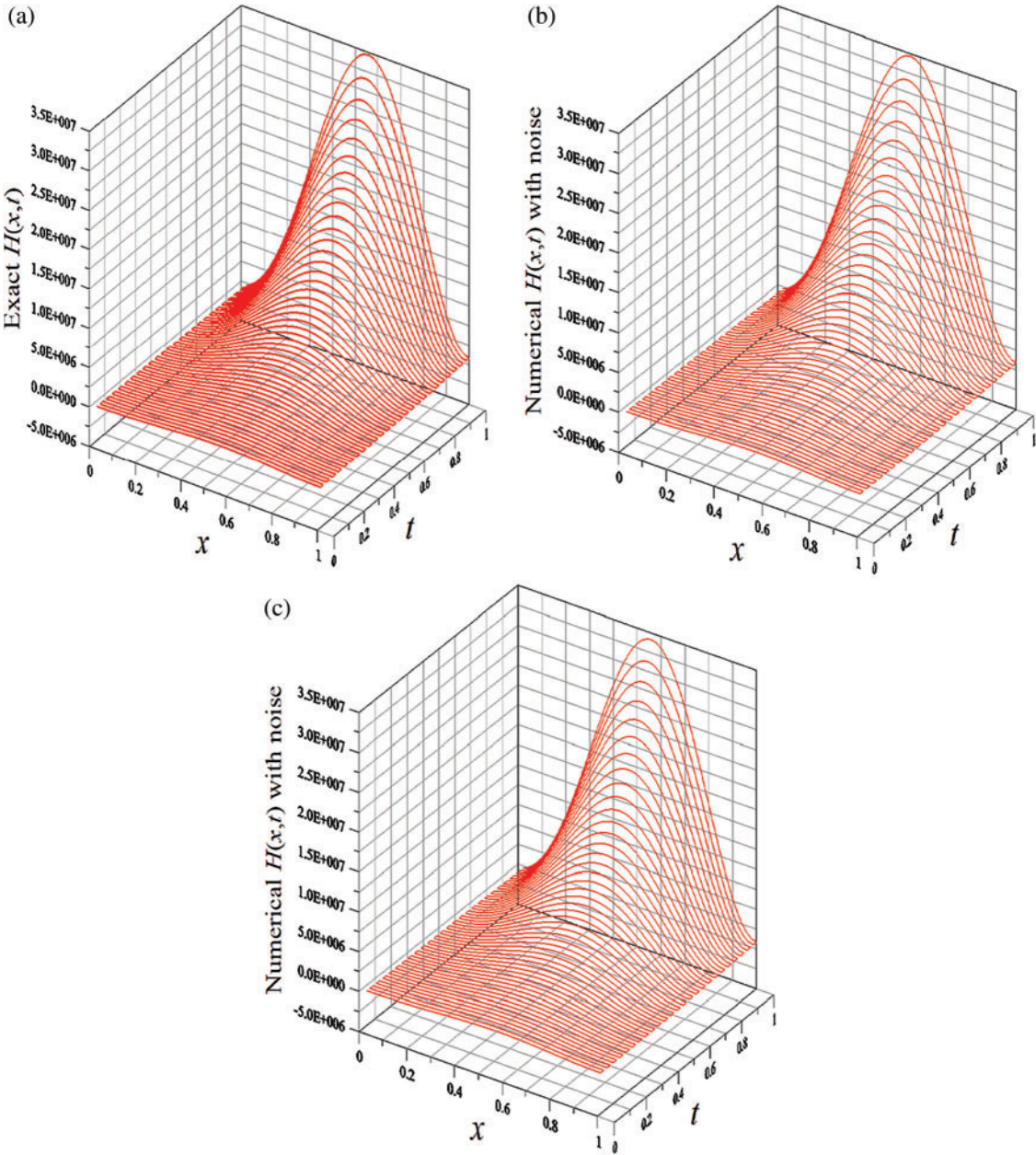


Figure 1: For example 1 of the unknown nonlinear force function, (a) displaying exact H , (b) numerical H with small noise $r = 0.9$, and (c) numerical recovery of H with large noise $\xi = 0.01$

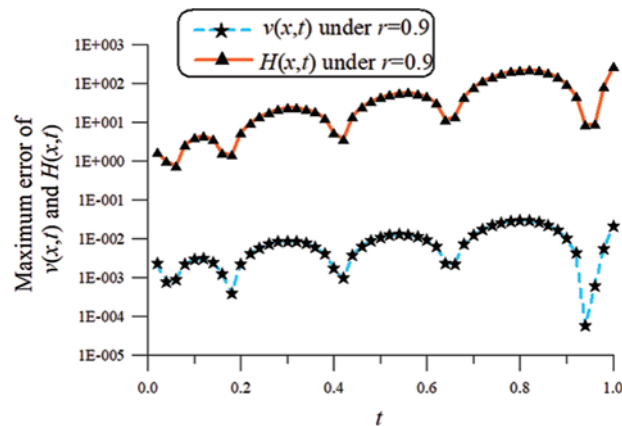


Figure 2: Example 1 resolved utilizing the BSFM and illustrating the maximum errors of v and the retrieved of H

The noise is $r = 0.2$, and we take $\beta = 1.5$. We employ the BSFM with $s = 3$ and $w = 200$. Comparing the numerically retrieved solution of $H(x, t)$ with the exact force $H(x, t)$, as displayed in Figs. 3a and 3c. We also illustrate the MEs of $v(x, t)$ and the recovery of $H(x, t)$ under the noisy effect in Fig. 4. Excellent results are acquired with the MEs over the plane $[0, 1] \times (0, 1]$ being 4.95 for $v(x, t)$ and 15039.55 for $H(x, t)$. We also reveal the maximum absolute value of $v(x, t)$ and $H(x, t)$ over the plane $[0, 1] \times (0, 1]$ is 1063.10 and 1.83×10^6 , respectively, and $e(H) = 7.11 \times 10^{-3}$ is small.

Deliberating a large relative noise of $\xi = 0.2$ in Eq. (40), we use the BSFM with $s = 3$ and $w = 200$ to retrieve $H(x, t)$, as shown in Fig. 3b. The accuracy compared with the aforementioned results is close, where the ME for $v(x, t)$ is 3.35, the ME for $H(x, t)$ is 15225.75, and $e(H) = 8.51 \times 10^{-3}$. For this instance, the CPU time is also less than 1.0 s.

4.3 Example 3 of A Cantilevered Beam

We demonstrate that the cantilevered beam has the boundary data, shape functions, and boundary shape functions as follows:

$$v(0, t) = 0, v_x(0, t) = 0, v_{xx}(l, t) = 0, v_{xxx}(l, t) = 0, \quad (46)$$

$$c_1(q, x) = 1 + \frac{ql^2}{(q+2)(q+3)} \bar{x}^{q+3} + \frac{x^2}{2} - \frac{l^2}{q+2} \bar{x}^{q+2},$$

$$c_2(q, x) = x + \frac{ql^2}{(q+2)(q+3)} \bar{x}^{q+3} + \frac{x^2}{2} - \frac{l^2}{q+2} \bar{x}^{q+2},$$

$$c_3(q, x) = -\frac{ql^2}{(q+2)(q+3)} \bar{x}^{q+3} + \frac{l^2}{q+2} \bar{x}^{q+2},$$

$$c_4(q, x) = -\frac{l^3}{(q+1)(q+2)} \bar{x}^{q+2} + \frac{l^3}{(q+2)(q+3)} \bar{x}^{q+3}, \quad (47)$$

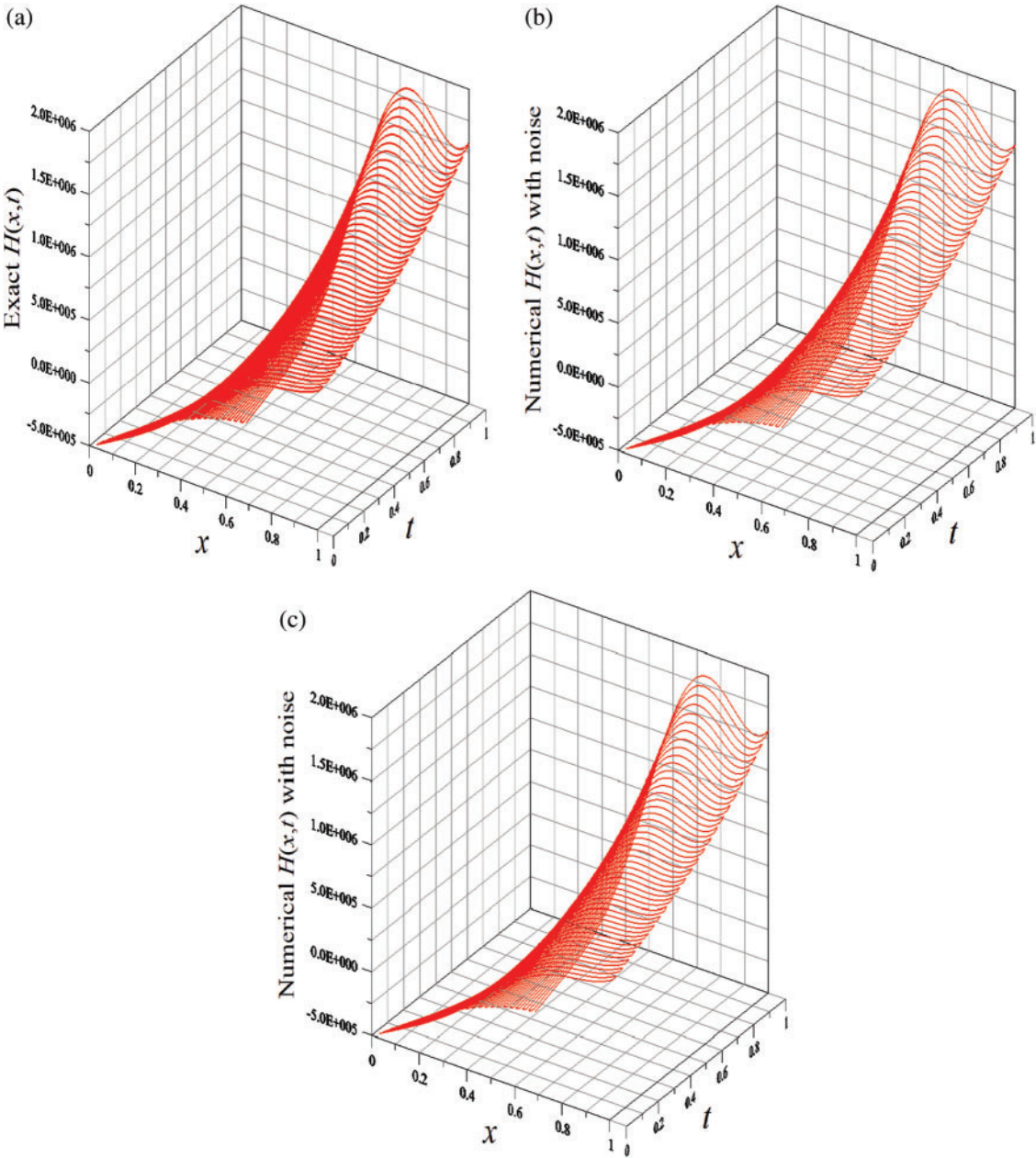


Figure 3: For example 2 of the unknown nonlinear force function, (a) displaying exact H , (b) numerical H with small noise $r = 0.2$, and (c) numerical recovery of H with large noise $\xi = 0.2$

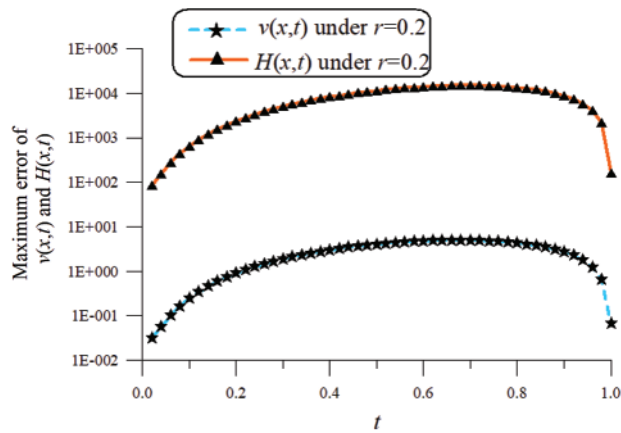


Figure 4: Example 2 resolved utilizing the BSFM and illustrating the maximum errors of v and the retrieved of H

$$D(q, x, t) = D^0(q, x, t) - c_1(q, x)D^0(q, 0, t) - c_2(q, x)D_x^0(q, 0, t) - c_3(q, x)D_{xx}^0(q, \ell, t) - c_4(q, x)D_{xxx}^0(q, \ell, t), \quad (48)$$

where $D^0(q, x, t)$ is depicted in Eq. (30).

We contemplate a nonseparable space-time-dependent force produced from

$$v(x, t) = 9 [t^2 \sin(\ell t) - \ell t^3 \cos(\ell t)] x^2 + 3t^3 \cos(\ell t) x^3 + e^t (18x^6 - 54\ell x^5 + 45\ell^2 x^4) + 18 \sin(xt) - 18xt. \quad (49)$$

The noise is $r = 0.9$, and we take $\beta = 5$. We utilize the BSFM with $s = 2$ and $w = 500$. Comparing the numerically retrieved solution of $H(x, t)$ with the exact force $H(x, t)$, as exhibited in Figs. 5a and 5c. We also display the MEs of $v(x, t)$ and the recovery of $H(x, t)$ under the noisy effect in Fig. 6. Good results are acquired with the MEs over the plane $[0, 1] \times (0, 1]$ being 0.18 for $v(x, t)$ and 103.27 for $H(x, t)$. We also indicate the maximum absolute value of $v(x, t)$ and $H(x, t)$ over the plane $[0, 1] \times (0, 1]$ is 25.94 and 15477.89, respectively, and $e(H) = 8.08 \times 10^{-3}$ is small.

Pondering a large relative noise of $\xi = 0.5$ in Eq. (40), we use the BSFM with $s = 3$ and $w = 200$ to retrieve $H(x, t)$, as shown in Fig. 5b. The accuracy compared with the aforementioned results is close, where the ME for $v(x, t)$ is 0.32, the ME for $H(x, t)$ is 125.60, and $e(H) = 4.68 \times 10^{-3}$. For this example, the CPU time is less than 1.0 s.

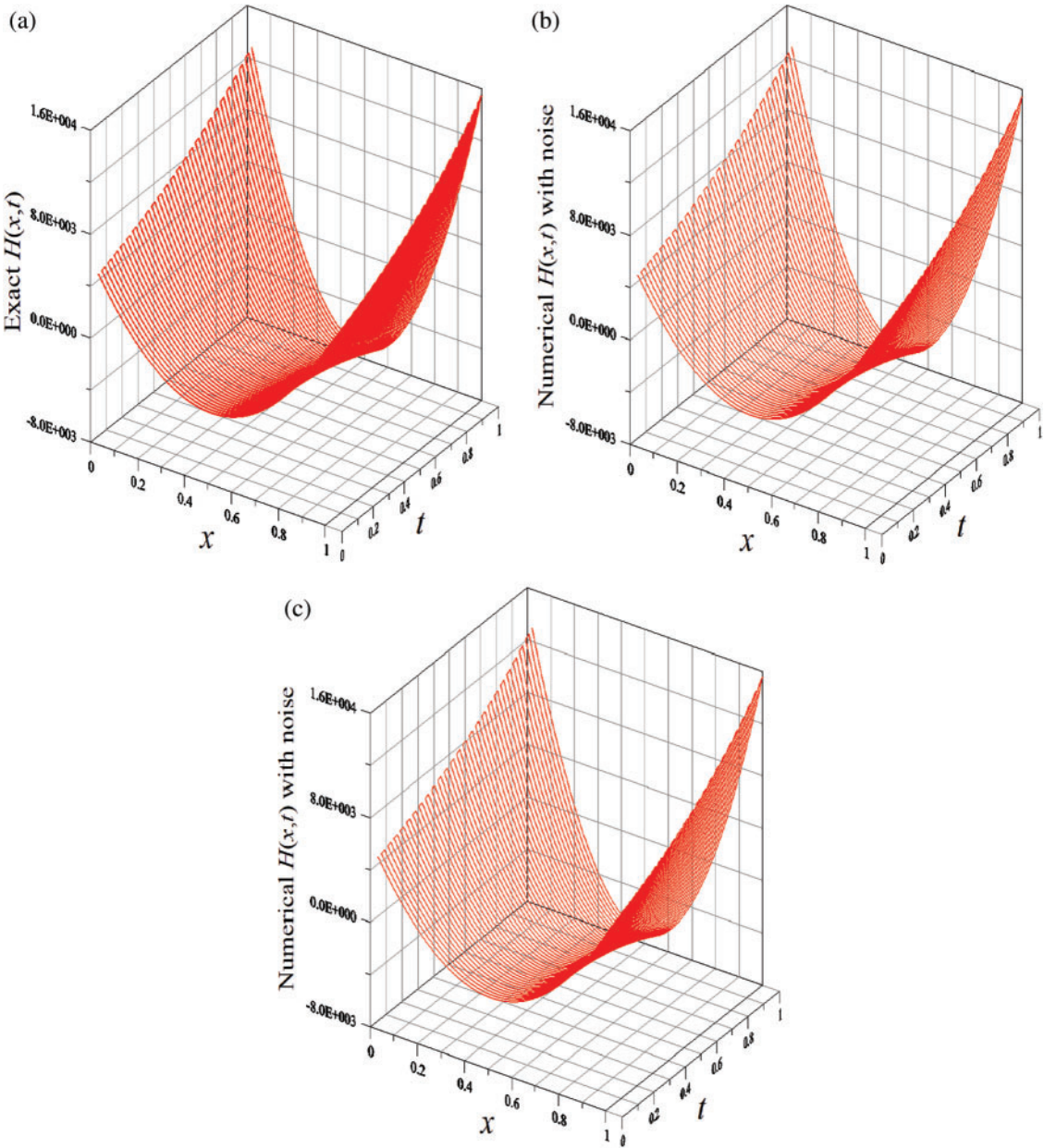


Figure 5: For example 3 of the unknown nonlinear force function, (a) displaying exact H , (b) numerical H with small noise $r = 0.9$, and (c) numerical recovery of H with large noise $\xi = 0.5$

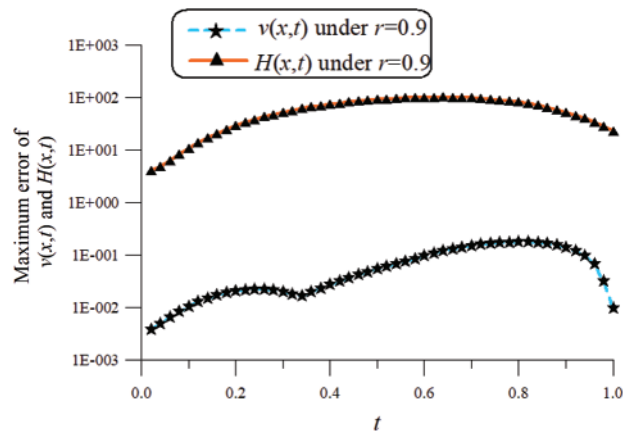


Figure 6: Example 3 resolved utilizing the BSFM and illustrating the maximum errors of v and the retrieved of H

4.4 Example 4 of A T wo-end Fixed Beam

For the two-end fixed beam we can calculate the boundary data, shape functions, and boundary shape functions as follows:

$$v(0, t) = 0, v_x(0, t) = 0, v(l, t) = 0, v_x(l, t) = 0, \tag{50}$$

$$\begin{aligned} c_1(q, x) &= 1 + (q + 1)\bar{x}^{q+2} - (q + 2)\bar{x}^{q+1}, \\ c_2(q, x) &= l [\bar{x} + q\bar{x}^{q+2} - (q + 1)\bar{x}^{q+1}], \\ c_3(q, x) &= (q + 2)\bar{x}^{q+1} - (q + 1)\bar{x}^{q+2}, \\ c_4(q, x) &= l[\bar{x}^{q+2} - \bar{x}^{q+1}], \end{aligned} \tag{51}$$

$$\begin{aligned} D(q, x, t) &= D^0(q, x, t) - c_1(q, x)D^0(q, 0, t) - c_2(q, x)D_x^0(q, 0, t) \\ &\quad - c_3(q, x)D^0(q, l, t) - c_4(q, x)D_x^0(q, l, t), \end{aligned} \tag{52}$$

where $D^0(j, x, t)$ is still described in Eq. (32).

In place of Eq. (5), we supply the moment condition at the right-hand side to the two-end fixed beam:

$$v_{xx}(l, t) = N(t). \tag{53}$$

Concurrently, we alter Eq. (38) to

$$\sum_{p=1}^n a_p D_{xx}(p, l, t_q) = N(t_q), q = 1, \dots, m. \tag{54}$$

Letting

$$\begin{aligned} v(x, t) &= t^2 (x^5 - 2lx^4 + l^2x^3) + 500 \cos(\pi t)(x^7 - 2lx^6 + l^2x^5) \\ &\quad + e^t [5 \exp(x^4 - 2lx^3 + l^2x^2) - 5] \end{aligned} \tag{55}$$

be an exact solution of the beam Eq. (1) under the boundary conditions in Eq. (50). The true function $H(x, t)$ can be obtained by introducing the above-mentioned $v(x, t)$ into Eq. (1).

The noise is $r = 0.9$, and we take $\beta = 0.2$. We use the BSFM with $s = 4$ and $w = 100$. Comparing the numerically retrieved solution of $H(x, t)$ with the exact force $H(x, t)$, as shown in Figs. 7a and 7c. We also demonstrate the MEs of $v(x, t)$ and the recovery of $H(x, t)$ under the noisy effect in Fig. 8. Good results are acquired with the MEs over the plane $[0, 1] \times (0, 1]$ being 8.18×10^{-2} for $v(x, t)$ and 60.68 for $H(x, t)$. We also exhibit the maximum absolute value of $v(x, t)$ and $H(x, t)$ over the plane $[0, 1] \times (0, 1]$ is 7.78 and 23989.37, respectively, and $e(H) = 2.47 \times 10^{-3}$ is small.

Considering a large relative noise of $\xi = 0.01$ in Eq. (40), we use the BSFM with $s = 8$ and $w = 100$ to retrieve $H(x, t)$, as presented in Fig. 7b. The accuracy compared with the above-mentioned results is close, in which the ME for $v(x, t)$ is 8.53×10^{-2} , the ME for $H(x, t)$ is 79.82, and $e(H) = 2.72 \times 10^{-3}$. For this instance, the CPU time is also less than 1.0 s.

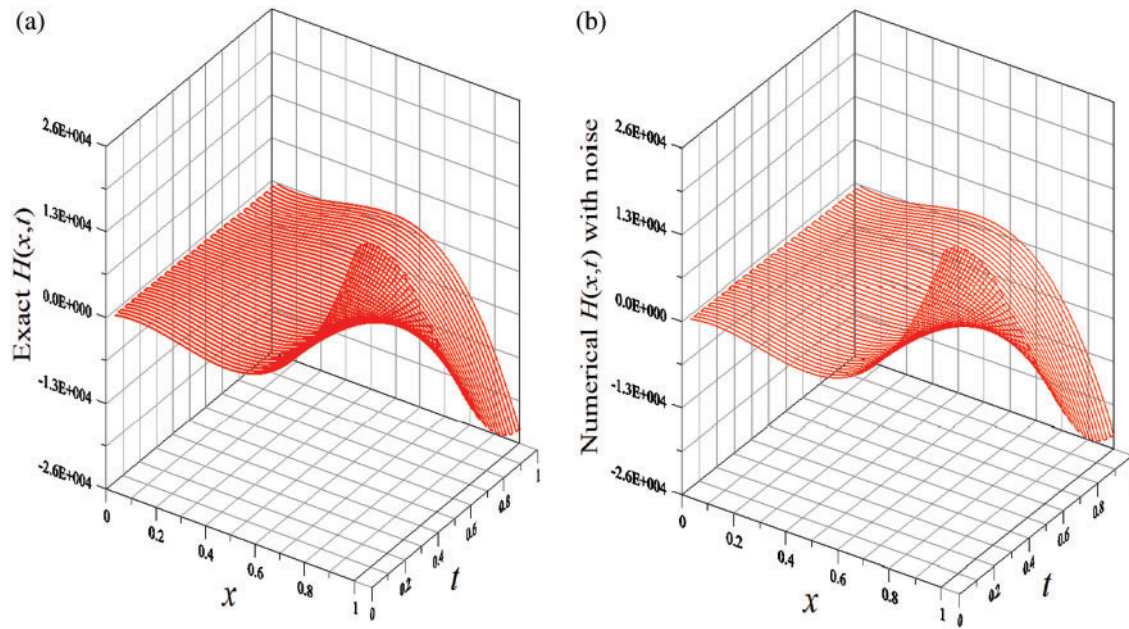


Figure 7: (Continued)

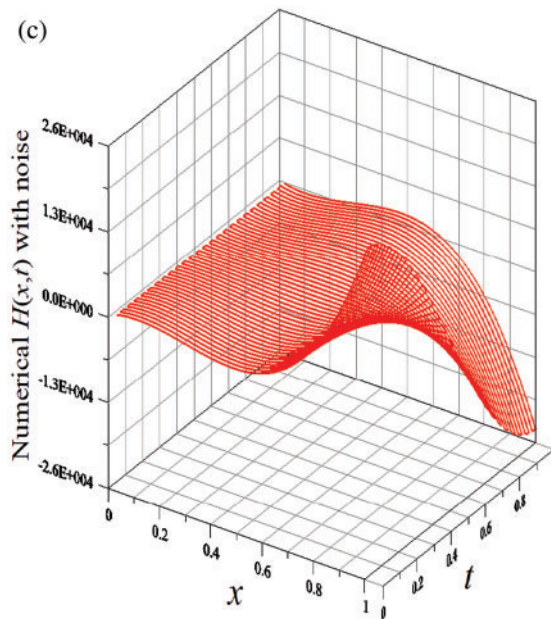


Figure 7: For example 4 of the unknown nonlinear force function, (a) displaying exact H , (b) numerical H with small noise $r = 0.9$, and (c) numerical recovery of H with large noise $\xi = 0.01$

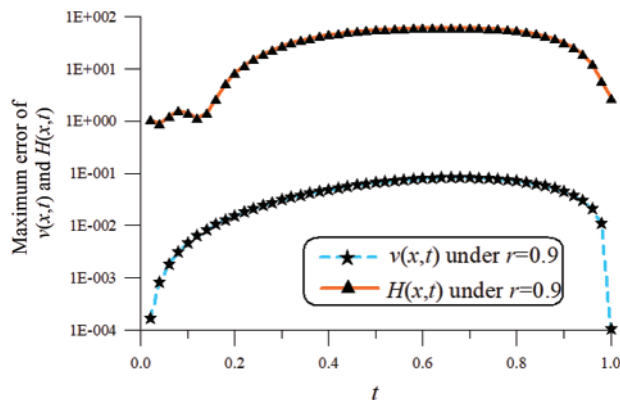


Figure 8: Example 4 resolved utilizing the BSFM and illustrating the maximum errors of v and the retrieved of H

5 Conclusions

We addressed the recovery issues of revealing unknown forces burdened with the nonlinear Euler-Bernoulli beams with four boundary-supported data, e.g., cantilevered, simply supported, two-end fixed, and clamped-hinged beams, by utilizing the boundary shape functions method. The innovation of this scheme is the establishment of a variety of boundary shape functions with varied orders for each beam sort, such that we have influential foundations from which to extend the solution in the whole space-time realm. The proposed scheme can be utilized in the online real-time estimation of unknown force functions in space-time for varied boundary supports of the vibrating beam. On the basis of those numerical examples, we display that the proposed algorithm is applicable to the nonlinear

external forces of nonlinear Euler-Bernoulli equations and pretty excellent computational efficiency, and even for adding the large random noise up to 50%. Furthermore, to the author's best knowledge, there has no report in the literature that the numerical schemes for those four issues can offer more accurate results than the present results. The present approach can be extended to cope with the multi-dimensional inverse nonlinear transient PDEs and will be worked out in the future.

Funding Statement: This work was financially supported by the National United University [grant numbers 111-NUUPRJ-04].

Conflicts of Interest: The author declares that he has no conflicts of interest to report regarding the present study.

References

- [1] S. M. Han, H. Benarova and T. Wei, "Dynamics of transversely vibrating beam using four engineering theories," *Journal of Sound and Vibration*, vol. 225, no. 5, pp. 935–988, 1999.
- [2] W. Y. Bao and I. N. Tansel, "Modelling micro-end-milling operations, Parts I and II," *International Journal of Machine Tools and Manufacture*, vol. 40, no. 15, pp. 2155–2192, 2000.
- [3] M. Abu-Hilal, "Forced vibration of Euler-Bernoulli beams by means of dynamic Green functions," *Journal of Sound and Vibration*, vol. 267, no. 2, pp. 191–207, 2003.
- [4] L. Andren, I. Hakansson, A. Brandt and I. Claesson, "Identification of motion of cutting tool vibration in a continuous boring operation—correlation to structural properties," *Mechanical Systems and Signal Processing*, vol. 18, no. 4, pp. 903–927, 2004.
- [5] M. C. Yoon and Y. G. Kim, "Cutting dynamic force modelling of end milling operation," *Journal of Materials Processing Technology*, vol. 155, no. 1, pp. 1383–1389, 2004.
- [6] J. Gradisek, M. Kalveram and K. Weinert, "Mechanistic identification of specific force coefficients for a general end mill," *International Journal of Machine Tools and Manufacture*, vol. 44, no. 4, pp. 401–414, 2004.
- [7] S. Nicaise and O. Zair, "Determination of point sources in vibrating beams by boundary measurements: identifiability, stability, and reconstruction results," *Electronic Journal of Differential Equations*, vol. 2004, no. 20, pp. 1–17, 2004.
- [8] M. Krstic, B. Z. Guo, A. Balogh and A. Smyshlyaev, "Control of a tip-force destabilized shear beam by observer-based boundary feedback," *SIAM Journal on Control and Optimization*, vol. 47, no. 2, pp. 553–574, 2008.
- [9] M. Krstic and A. Smyshlyaev, *Boundary control of PDEs: A course on backstepping designs*. Philadelphia: SIAM, 2008.
- [10] A. Hasanov, "Identification of an unknown source term in a vibrating cantilevered beam from final overdetermination," *Inverse Problems*, vol. 25, no. 11, pp. 115015, 2009.
- [11] C. H. Huang, C. C. Shih and S. Kim, "An inverse vibration problem in estimating the spatial and temporal-dependent external forces for cutting tools," *Applied Mathematical Modelling*, vol. 33, no. 6, pp. 2683–2698, 2009.
- [12] C. S. Liu, "A Lie-group adaptive differential quadrature method to identify unknown force in an Euler-Bernoulli beam equation," *Acta Mechanica*, vol. 223, no. 10, pp. 2207–2223, 2012.
- [13] A. Kawano, "Uniqueness in the identification of asynchronous sources and damage in vibrating beams," *Inverse Problems*, vol. 30, no. 6, pp. 065008, 2014.
- [14] A. Hasanov and O. Baysal, "Identification of an unknown spatial load distribution in a vibrating cantilevered beam from final overdetermination," *Journal of Inverse and Ill-posed Problems*, vol. 23, no. 1, pp. 85–102, 2015.
- [15] A. Hasanov and A. Kawano, "Identification of unknown spatial load distributions in a vibrating Euler-Bernoulli beam from limited measured data," *Inverse Problems*, vol. 32, no. 5, pp. 055004, 2016.

- [16] A. Hasanov and O. Baysal, "Identification of unknown temporal and spatial load distributions in a vibrating Euler-Bernoulli beam from Dirichlet boundary measured data," *Automatica*, vol. 71, no. 3, pp. 106–117, 2016.
- [17] A. Maciag and A. Pawinska, "Solution of the direct and inverse problems for beam," *Computational and Applied Mathematics*, vol. 35, no. 1, pp. 187–201, 2016.
- [18] C. S. Liu and B. Li, "An upper bound theory to approximate the natural frequencies and parameters identification of composite beams," *Composite Structures*, vol. 171, pp. 131–144, 2017.
- [19] C. S. Liu, W. S. Jhao and C. W. Chang, "A simple non-iterative method for recovering a space-dependent load on the Euler-Bernoulli beam equation," *Mathematical Methods in the Applied Sciences*, vol. 41, no. 17, pp. 7641–7654, 2018.
- [20] C. S. Liu, L. Qiu and F. Wang, "Nonlinear wave inverse source problem solved by a method of m-order homogenization functions," *Applied Mathematics Letters*, vol. 91, pp. 90–96, 2019.
- [21] C. S. Liu, L. Qiu and L. Lin, "Solving the higher-dimensional nonlinear inverse heat source problems by the superposition of homogenization functions method," *International Journal of Heat and Mass Transfer*, vol. 141, pp. 651–657, 2019.
- [22] J. M. Bajkowski, B. Dyniewicz, M. Gebik-Wrona, J. Bajkowski and C. I. Bajer, "Reduction of the vibration amplitudes of a harmonically excited sandwich beam with controllable core," *Mechanical Systems and Signal Processing*, vol. 129, no. 8, pp. 54–69, 2019.
- [23] C. S. Liu, L. Qiu and L. Lin, "Simulating thin plate bending problems by a family of two-parameter homogenization functions," *Applied Mathematical Modelling*, vol. 79, no. 1, pp. 284–299, 2020.
- [24] J. Peng, M. Xiang, L. Wang, X. Xie, H. Sun *et al.*, "Nonlinear primary resonance in vibration control of cable-stayed beam with time delay feedback," *Mechanical Systems and Signal Processing*, vol. 137, no. 3, pp. 106488, 2020.
- [25] M. Li, S. Du, F. Li and X. Jing, "Vibration characteristics of novel multilayer sandwich beams: Modelling, analysis and experimental validations," *Mechanical Systems and Signal Processing*, vol. 142, no. 5, pp. 106799, 2020.
- [26] H. Arvin, A. Arena and W. Lacarbonara, "Nonlinear vibration analysis of rotating beams undergoing parametric instability: lagging-axial motion," *Mechanical Systems and Signal Processing*, vol. 144, no. 6, pp. 106892, 2020.
- [27] C. S. Liu, C. L. Kuo and C. W. Chang, "Recovering external forces on vibrating Euler-Bernoulli beams using boundary shape function methods," *Mechanical Systems and Signal Processing*, vol. 148, pp. 107157, 2021.
- [28] A. Barari, H. D. Kaliji, M. Ghadimi and G. Domairry, "Non-linear vibration of Euler-Bernoulli beams," *Latin American Journal of Solids and Structures*, vol. 8, no. 2, pp. 139–148, 2011.
- [29] O. Weeger, U. Wever and B. Simeon, "Isogeometric analysis of nonlinear Euler-Bernoulli beam vibrations," *Nonlinear Dynamics*, vol. 72, no. 4, pp. 813–835, 2013.
- [30] S. Kitarovic, "Nonlinear Euler-Bernoulli beam kinematics in progressive collapse analysis based on the Smith's approach," *Marine Structures*, vol. 39, no. 12, pp. 118–130, 2014.
- [31] S. Bagheri, A. Nikkar and H. Ghaffarzadeh, "Study of nonlinear vibration of Euler-Bernoulli beams by using analytical approximate techniques," *Latin American Journal of Solids and Structures*, vol. 11, no. 1, pp. 157–168, 2014.
- [32] A. Raza, J. Awrejcewicz, M. Rafiq, N. Ahmed, M. S. Ehsan *et al.*, "Dynamical analysis and design of computational methods for nonlinear stochastic leprosy epidemic model," *Alexandria Engineering Journal*, vol. 61, no. 10, pp. 8097–8111, 2022.
- [33] A. Raza, M. Rafiq, D. Alrowaili, N. Ahmed, I. Khan *et al.*, "Design of computer methods for the solution of cervical cancer epidemic model," *CMC: Computers, Materials & Continua*, vol. 70, no. 1, pp. 1649–1666, 2022.
- [34] K. Abodayeh, A. Raza, M. Rafiq, M. S. Arif, M. Naveed *et al.*, "Analysis of pneumonia model via efficient computing techniques," *CMC: Computers, Materials & Continua*, vol. 70, no. 3, pp. 6073–6088, 2022.

- [35] A. Raza, D. Baleanu, M. Rafiq, S. Z. Abbas, A. Siddique *et al.*, “Computational algorithms for the analysis of cancer virotherapy model,” *Computers, Materials & Continua*, vol. 71, no. 2, pp. 3621–3634, 2022.
- [36] A. Raza, E. E. Mahmoud, A. M. Al-Bugami, D. Baleanu, M. Rafiq *et al.*, “Examination of pine wilt epidemic model through efficient algorithm,” *Computers, Materials & Continua*, vol. 71, no. 3, pp. 5293–5310, 2022.
- [37] A. Raza, M. Rafiq, J. Awrejcewicz, N. Ahmed and M. Mohsin, “Dynamical analysis of coronavirus disease with crowding effect, and vaccination: a study of third strain,” *Nonlinear Dynamics*, vol. 107, no. 4, pp. 3963–3982, 2022.